2019 CMBEC42
Ottawa, ON
CMBES/SCGB May 21-24, 2019

Automatic C-arm Positioning Using Multi-Functional User Interface

M. Haiderbhai[1], J. Guerrero Turrubiates[1], Vinod Gutta[2] and P. Fallavollita[2]

[1]Interdiscplinary School of Health Sciences, University of Ottawa, Ottawa, Canada

Abstract— **C-arm positioning is a critical step of the surgical workflow. The traditional method is often time consuming and results in additional radiation exposure to the patient and surgical staff. We propose a user interface that allows surgeons to interact with a simulated X-ray 3D reconstruction of the patient's anatomy. Optimal views chosen by the surgeon with the simulated X-ray are used to calculate the C-arm position required to achieve that view. The proposed system uses pre-operative CT data to generate a 3D model, and inverse kinematics with 6 degrees of freedom to calculate the C-arm joint parameters. Day of surgery patient position variations are factored in through registration methods using the Kinect. Quantitative results were validated by comparing outputs with ground truths, and results indicate our method can output C-arm position values close to the truth considering the limitation of working with truncated values. Automatic positioning reduces radiation by minimizing typical positioning errors. Future work will include the integration of radiation exposure measurements and visualization into the user interface.**

Keywords— **Inverse Kinematics, C-arm, X-ray, Patient Registration, User Interface.**

I. Introduction

Mobile C-arm devices are used in a variety of modern surgeries and require the positioning of the C-arm by surgical staff to facilitate surgical navigation. The current method relies on the expertise of the surgical staff, however, due to the uniqueness of each patient's body, surgical team miscommunication, inexperience, and other uncontrollable factors, the positioning often requires acquisition of multiple X-rays before reaching the desired view that the surgeon requires [1]. This method exposes the patient and all nearby surgical staff to large doses of radiation and time loss that could be avoided [2].

Previous work has proven the theoretical viability that the C-arm position can be calculated using the region of interest and the beam direction [3]. This inverse kinematic approach allows for the positioning of the C-arm by inputting the parameters of the end beam outcome. The application of such an approach has been shown through virtual reality guided positioning, useful for training staff [4]. The key factor in achieving clinical relevance is the ability to visualize the hidden anatomy of the patient prior to surgery and maintain accuracy so that the proposed C-arm position delivers the exact image. Other works have clinically tested the use of pre-operative CT images to simulate the X-ray view, allowing surgeons to manipulate and choose their X-ray desired view [5]. The study implementation was tested during surgery, and results were positive that the output joint parameters allowed for quick C-arm positioning that matched the views picked pre-operatively with minimal error.

We propose a user interface that uses pre-operative CT images to mimic the C-arm X-ray view, which can be used by surgeons to find their desired views. In this way, the surgeon can directly choose the outcome of the C-arm X-rays without worrying about the complex issues with positioning. These views can be used in an inverse kinematic calculation to determine the C-arm position. Our approach uses 6 degrees of freedom, greater than what has previously been accomplished, to allow for more flexibility and range of motion for the C-arm positions. Patient registration prior to surgery can help increase the accuracy of positioning by considering deviations from the body position during the CT scan.

II. Methodology

A. DICOM image viewer and 3D reconstruction

The prototype was created in Unity and programmed in C#. With the help of the open source software ITK, DICOM images of the patient can be loaded into the application and are used to create a patient specific simulation. The data from these DICOM images is extracted to give patient information and image data. The image data is reconstructed to create the typical three plane views that physicians require; coronal, transverse, and sagittal. The 3D pixel volume is then segmented using dual threshold segmentation to isolate vascular. We use aortic aneurysms as an example clinical focus, so the segmentation isolates the main arteries from nearby tissue. This volume is then converted to a 3D model using a volume to mesh generation algorithm. This 3D model can then be used in the views portion of the interface.

B. Inverse Kinematics

In order to obtain the C-arm position, a set of equations to perform the inverse kinematics must be determined. Figure 1 shows the point of interest and a blender model of the C-arm joints used to obtain the mathematical model. In this model, the six degrees of freedom are: movement of the base in the x-axis, movement of the base in the y-axis, height change in the z axis, wig-wag rotation with respect to the z-axis from the base, tilt rotation of the C around the x axis, orbital rotation of the C around the y axis.

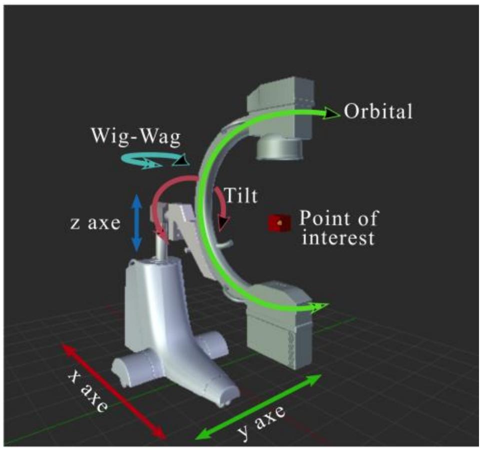

Fig. 1 Point of interest in the C-arm

Figure 2 displays the model of the five joints in order to obtain six degrees of freedom. This configuration allows the C-arm to be positioned with any arbitrary coordinates, being constrained only by the physical restrictions of the device itself. The input to the mathematical model will be the set of coordinates and rotations {x, y, z, $\theta_{\text{Wig-wag}}$, θ_{Tilt}, θ_{Orbital}} from the point of interest. Table 1 shows the Denavit-Hartenberg parameters [7] used to build the inverse kinematics model.

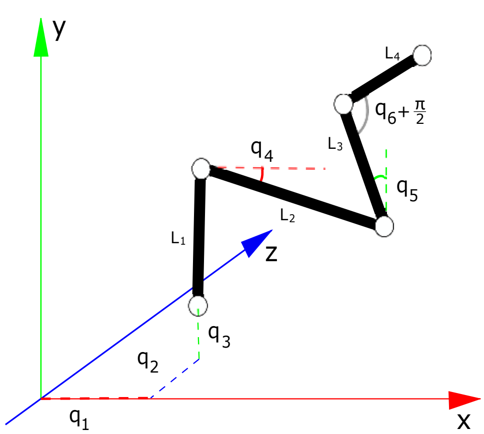

Fig. 2 Modeled C-arm

Table 1 Denavit-Hartenberg parameters for the C-arm

Joint	θ	d	a	α
1	0	0	q_1	0
2	π/2	0	q_2	0
3	0	L_1+q_3	0	π/2
4	$-\pi/2+q_4$	0	0	$-\pi/2+q_4$
5	$-\pi/2+q_5$	L_2	L_3	π/2
6	$\pi/2+q_6$	0	L_4	- π/2

Several tests were performed to evaluate quantitatively the results obtained from the inverse kinematics equations. These tests were implemented by first considering the coordinates and the three rotations of the point of interest (*user values*). Then, applying the inverse kinematics equations we obtained the output parameters $\mathbf{q_n}$, where *n* represents a joint index as shown in Figure 2. To verify that the result is correct, forward kinematics was performed by using the same $\mathbf{q_n}$ parameters. This should theoretically return the same coordinates and rotations of the point of interest (*computed values*). The test was performed 1000 times using Matlab® on a Macbook Pro 2.5 GHz Intel Core i5 to verify the difference between the user values and the computed values using forward kinematics.

C. Patient Registration

To minimize variation between the patient position during the CT scan and during the operation, patient registration was incorporated into interface. The application is connected to a Kinect that would ideally be mounted on the C-arm device, close to the X-ray source. A point cloud taken from the Kinect of the patient's body on the surgical table, and a second point cloud generated from the surface body of the CT scan is compared. Rigid, affine, and non-rigid registration methods using the Coherent Point Drift algorithm developed by Myronenko et al [6] is used to generate a transformation matrix T that consists of a translation vector and rotation matrix. These values can then be integrated into the inverse kinematic equation chain to determine the necessary adjustments to the C-arm joint parameters. The algorithms were validated by applying the translation and rotation manually, and then inputting the result to the algorithm to see if it can determine what transformations were applied. This method still used a Kinect generated point cloud and CT generated point cloud even though the transformation was manually applied. Four possible methods of registration were compared: rigid without scaling, rigid with scaling, affine, and non-rigid registration.

III. RESULTS

Figure 3 shows the user interface for the DICOM tab. Here the DICOM images are loaded by entering a file path, and slices from all three planes are shown. On the right, the output of the CT image data to 3D model is shown. This model will be used in the next portion of the interface.

Fig 3. DICOM view tab of the user interface

Figure 4 showcases the main feature of the interface, the ability to choose your desired views. On the left is an interactive X-ray simulation that can be manipulated by touch or mouse by the surgeon to rotate the model. Alternatively, specific values can be inputted in the middle input area. The right model shows a simulation of the results of the inverse kinematic equations. The calculations are done instantly to provide a fluid interactive experience.

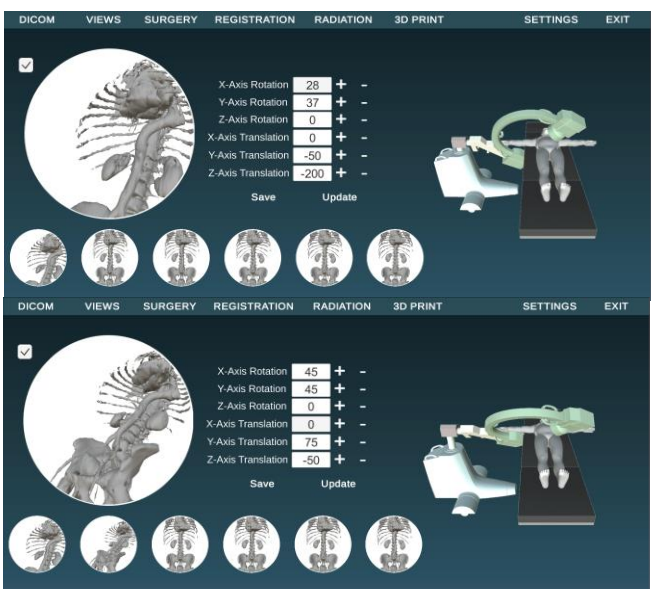

Fig 4. Two samples of the Views tab of the user interface

Table 2 Example of inverse kinematics outputs (q_n parameters) using input user values

variable	x	y	z	$\theta_{Wig'Wag}$	θ_{Tilt}	$\theta_{Orbital}$
user	1.0	0.7	2.0	0	30	0
computed	0.97854	0.13342	1.7791	0	30	0

Table 3 Example of forward kinematics to output user values

variable	q_x	q_y	q_z	$q_{\theta Wig'Wag}$	$q_{\theta Tilt}$	$q_{\theta Orbital}$
computed	0.97854	0.13342	1.7791	0	30	0
user	0.93613	0.7	1.9894	0	30	0

An example of the comparison between inverse and forward kinematics is shown in Tables 2 and 3. Table 2 shows the user values for coordinates and rotations, as well as the inverse kinematics computed values result. Table 3 shows the computed values as input to perform the calculation to get back to coordinates and rotations. The result should be equal to those of the user values in Table 2.

Patient registration was validated by examining resulting point cloud and matrices. Standard deviations were calculated by calculating the difference between the input transformation matrix and the output matrix. Table 4 displays the standard deviations achieved through each registration method.

Table 4. Standard deviations results of each registration method

	Rigid without scaling	Rigid with scaling	Affine	Non-rigid
No transformation	0.0121	0.0067	0.0018	0.0006
Only translation	0.0121	0.0067	0.0018	0.0006
Translation and rotation.	0.0122	0.0067	0.0018	0.0006

Visual results of non-rigid registrations are visualized in Figure 5. Here, the near perfect overlapping of the point clouds indicates a successful registration, which corresponds to the low standard deviation seen in Table 4.

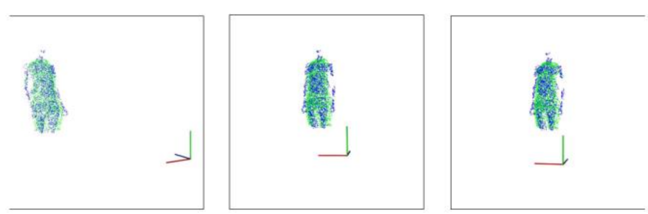

Figure 5. Results of non-rigid registration between original point cloud (blue) and registered point cloud (green).

IV. Discussion

The successful prototype showcases the entire workflow from inputting CT data to outputting C-arm positions. The inverse kinematic approach can output C-arm positions for all combinations of input parameters that fall within the threshold range of allowable values. Registration can detect variation in position and rotation between point clouds with a low standard deviation, and this transformation matrix can be used to increase the accuracy of results on the day of the surgery. The significance of our design is the complete integration of many different features that together increases the clinical relevancy of the prototype. Previous work used pre-generated models, however, views generated from one patient might not be relevant or optimal for the next [5]. By using pre-operative CT scans to generate our anatomical models and views, we ensure that the surgeon is viewing relevant data, providing increased clinical benefit.

The study uses inverse kinematics to determine C-arm position, and forward kinematics to compare the results. The obtained results show that the error rate is between 3 to 7 percent of the user values. This is due to the rounding of values in computers. Since our algorithms are based on trigonometric functions, the computed values are truncated as we are using a maximum of 5 digits to compute values such as sin (θ). The validation of the inverse kinematics by using real parameters will be explored as future work, as well as improving the approach to eliminate these errors. Compared to the 2 to 5 degrees of freedom used in previous studies, we broadened our approach to 6 degrees of freedom, allowing us to calculate a wider range of C-arm positions. In the future we hope to increase our approach to 9 degrees of freedom, integrating the surgical table into the equation, which will allow us to achieve an almost complete range of motion of position possibilities.

Finally, the integration of registration methods into our calculations was critical to increasing accuracy. The results show that non-rigid registration methods, which have the lowest standard deviation, should be used in the final implementation. In the future, the registration will be validated in the clinical environment using an actual C-arm.

There are a few limitations to the protype that are currently being improved. The current method uses a 3D reconstruction as the X-ray simulation. This methodology does not achieve the similarity to the X-ray that would be expected, and so a necessary improvement that is being made is the integration of digitally reconstructed radiography. This method uses ray casting algorithms similar to how an X-ray functions to generate digital images similar to X-rays. Integrating this functionality will make it easier for surgeons to envision the view they have in mind, as the simulation will more closely resemble the X-ray outcome of a C-arm.

V. Conclusion

The integration of CT images, inverse kinematics, and body registration into a complete user interface package is a key step in accomplishing the perfect clinical C-arm positioning tool. These initial steps lay the foundation to develop and prepare the interface for clinical studies, where the data collected will be vital to perfecting our approach for clinical use. This interface will also allow us to capture the knowledge of surgeon's and experienced staff in a way that can be quantifiable for future use in artificial intelligence. This work will hopefully revolutionize the current methodology used in the surgical workflow, ultimately benefitting both the patient and surgical staff.

Conflict of Interest

The authors declare that they have no conflict of interest.

References

1. Reiser, E. W., Desai, R. A., Byrd, S. S., Farber, H. E., Chi, D., Idler, C., & Isaacs, R. (2017). C-arm Positioning Is a Significant Source of Radiation in Spine Surgery. SPINE, 42(9), 707-710.
2. De Silva, T., Punnoose, J., Uneri, A., Goerres, J., Jacobson, M., Ketcha, M. D., Manbachi, A., Vogt, S., Kleinszig, G., Khanna, A. J., Wolinksy, J. P., Osgood, G., … Siewerdsen, J. H. (2017). C-arm Positioning Using Virtual Fluoroscopy for Image-Guided Surgery. Proceedings of SPIE--the International Society for Optical Engineering, 10135, 101352K.
3. Matthäus, L., Binder, N., Bodensteiner, C., & Schweikard, A. (2007). Closed-form inverse kinematic solution for fluoroscopic C-arms. Advanced Robotics, 21(8), 869-886.
4. Zhenzhou Shao, Yong Guan, & Jindong Tan. (2014). Virtual Reality Aided Positioning of Mobile C-arms for Image-Guided Surgery. Advances in Mechanical Engineering, 6(10), 1-14.
5. Fallavollita, P., Winkler, A., Habert, S., Wucherer, P., Stefan, P., Mansour, R., ... & Navab, N. (2014, September). Desired-view controlled positioning of angiographic C-arms. In International Conference on Medical Image Computing and Computer-Assisted Intervention (pp. 659-666). Springer, Cham.
6. Myronenko, & Xubo Song. (2010). Point Set Registration: Coherent Point Drift. Pattern Analysis and Machine Intelligence, IEEE Transactions on, 32(12), 2262-2275.
7. Denavit J. & Hartenberg S. (1955). A kinematic notation for lower-pair mechanisms based on matrices. Trans ASME J. Appl. Mech. 23, 215-221.

Corresponding author:

Author: Mustafa Haiderbhai
Institute: Interdisciplinary School of Health Sciences. Faculty of Health Sciences, University of Ottawa.
Street: 200 Lees Avenue
City: Ottawa
Country: Canada
Email: mhaid008@uottawa.ca